



# Storage and source of polycyclic aromatic hydrocarbons in sediments downstream of a major coal district in France



O. Bertrand <sup>a, b, \*</sup>, L. Mondamert <sup>c</sup>, C. Grosbois <sup>a</sup>, E. Dhivert <sup>a</sup>, X. Bourrain <sup>d</sup>, J. Labanowski <sup>c</sup>, M. Desmet <sup>a</sup>

<sup>a</sup> Université François Rabelais de Tours, EA 6293 GêHCO, Parc de Grandmont, 37200 Tours, France

<sup>b</sup> CNRS/INSU, ISTO, UMR 7327, 45071 Orléans, France

<sup>c</sup> Université de Poitiers, UMR 7285 IC2MP, 4 rue Michel Brunet, 86022 Poitiers Cedex, France

<sup>d</sup> Agence de l'Eau Loire-Bretagne, 9 Avenue Buffon, CS 36339, 45063 Orléans Cedex 2, France

## ARTICLE INFO

### Article history:

Received 29 April 2015

Received in revised form

7 September 2015

Accepted 9 September 2015

Available online xxx

### Keywords:

Polycyclic aromatic hydrocarbon  
Coal district  
Sediment core  
Bed sediments  
Loire river

## ABSTRACT

During the 20th century, the local economy of the Upper Loire Basin (ULB) was essentially based on industrial coal mining extraction. One of the major French coal districts with associated urban/industrial activities and numerous coking/gas plants were developed in the Ondaine-Furan subbasins, two tributaries of the upper Loire main stream. To determine the compositional assemblage, the level and the potential sources of contamination, the historical sedimentary chronicle of the 16 US EPA priority polycyclic aromatic hydrocarbons (PAHs) has been investigated. PAH concentrations were determined using gas chromatography/mass spectrometry (GC/MS) in a dated core, sampled in the Villerest flood-control reservoir located downstream of the Ondaine-Furan corridor (OFC). The most contaminated sediments were deposited prior to 1983 ( $\Sigma 16\text{PAHs}$  ca. 4429–13,348 ng/g) and during flood events ( $\Sigma 16\text{PAHs}$  ca. 6380 ng/g – 1996 flood; 5360 ng/g – 2003 flood; 6075 ng/g – 2008 flood), especially in medium and high molecular weight PAHs. Among them, typical pyrogenic PAHs such as FLT, PYR, BbF and BaP were prevalent in most of the core samples. In addition, some PAHs last decade data is available from the Loire Bretagne Water Agency and were analyzed using high-performance liquid chromatography with postcolumn fluorescence derivatization (HPLC/FLD). These results confirm that the most highly contaminated sediments were found downstream of OFC ( $\Sigma 16\text{PAHs}$  ca. 2264–7460 ng/g). According to the observed molecular distribution, PAHs are originated largely from high-temperature pyrolytic processes. Major sources of pyrogenic PAHs have been emphasized by calculation of specific ratios and by comparison to reported data. Atmospheric deposition of urban and industrial areas, wood combustion and degraded coal tar derived from former factories of coking/gas plants seem to be the major pyrogenic sources. Specifically, particular solid transport conditions that can occur during major flood events lead us to emphasize weathering of former contamination sources, such as more preserved coal tar.

© 2015 Elsevier Ltd. All rights reserved.

## 1. Introduction

Polycyclic aromatic hydrocarbons (PAHs) have received particular attention because of their widespread accumulation in soils, sediments and waters and their associated toxic, carcinogenic and mutagenic risks (Lehr and Jerina, 1977; White, 1986; Zedeck, 1980). PAHs found in aquatic environments are generally strongly sorbed onto organic and inorganic suspended particles because of their

low water solubilities (Karcher, 1988). Thus, sediments are one of the most important PAH reservoirs (Landrum and Robbins, 1990; Readman et al., 1984). A vast number of publications reports the presence of PAHs in river sediment (Doong and Lin, 2004; Fernandes et al., 1997; Fu et al., 2011; Gocht et al., 2001; Ko et al., 2007; Xu et al., 2007), lakes (Choudhary and Routh, 2010; Grimalt et al., 2004; Guo et al., 2010, 2011; Jung et al., 2008) or marine environments (Pereira et al., 1996; Qiao et al., 2006; Soclo et al., 2000; Witt, 1995). Thus, the United States Environmental Protection Agency (U.S. EPA) has listed 16 of these PAHs on their priority-pollutant list.

PAHs may have different sources, which are primarily

\* Corresponding author. CNRS/INSU, ISTO, UMR 7327, 45071 Orléans, France.  
E-mail address: [olivia.bertrand@cnrs-orleans.fr](mailto:olivia.bertrand@cnrs-orleans.fr) (O. Bertrand).

anthropogenic. The pyrogenic origin is one of the major sources of PAHs (Mc Elroy et al., 1989). More precisely, PAHs with four to six rings are generally formed through incomplete combustion of recent and fossil organic matter at high temperature during anthropogenic activities, such as burning of fossil-fuels, vehicular emissions, combustion processes of solid incineration plant and domestic heating (Dahle et al., 2003; Sanders et al., 2002; Yunker et al., 2002), but also during natural processes, such as forest and prairie fires (Lafamme and Hites, 1978). These pyrogenic PAHs can be dispersed over long distances in the atmosphere and then deposited by wet and dry deposition (Cranwell and Koul, 1989). In contrast, significant sources of PAHs with two or three rings derived from petrogenic contamination are offshore petroleum hydrocarbon production and/or petroleum exportation. A well-known approach to characterize the predominant sources of PAHs is the use of relative PAH ratios considering isomers formed by different processes (Yunker et al., 2002). These ratios are based on the relative thermodynamic stability of some PAH isomers. The thermodynamics of the pyrogenic and petrogenic formation of PAHs lead to the release of two different classes of isomers. The isomers called “kinetic” are mainly generated during combustion at elevated temperature and have a low relative stability. In contrast, “thermodynamic” isomers have higher relative stability and are produced at low temperatures during long duration processes such as diagenesis or catagenesis (Budzinski et al., 1997; Yunker et al., 2002).

Until now, historical records of PAH pollution were largely derived from lake and sea sediment core studies (Fernandez et al., 2000; Grimalt et al., 2004; Guo et al., 2006; Itoh et al., 2010; Jung et al., 2008; Xu et al., 2014), whereas results of similar investigations of European fluvial systems have been scarcely reported (Gocht et al., 2001; Ayrault et al., 2008; Micic et al., 2013). One of the main reasons for this lack is the difficulty of finding continuous and undisturbed records over several decades in industrialized basins. Then, no study has yet investigated the distribution and sources of PAHs in the Upper Loire Basin (ULB) bed sediments, although it includes one of the major French coal districts. Currently, few studies have also reported PAHs contamination from industrialized and urbanized regions associated to coke production in aquatic systems (Li et al., 1998; Gu et al., 2003; Christensen and Bzdusek, 2005). Then, the objectives of the present study are (i) to make an environmental assessment of the historical record of the Villerest flood-control reservoir to expand its potential for the reconstruction of the PAHs contamination over the last thirty years, (ii) to compare this contamination to some PAHs data obtained from a broader context of the ULB bed sediments (iii) to identify the possible sources of PAHs in order to understand the environmental quality of large fluvial systems close to coal districts.

## 2. Material and methods

### 2.1. Description of the study area

The sampling area is located in the upstream part of the Loire basin. The Loire river is the largest river in France (1012 km) and the upper section is 448 km long with a drainage area of 17,570 km<sup>2</sup> (15% of the total basin area). The coal district is located in the Ondaine-Furan corridor (OFC), two small tributaries of the upper Loire main stream (Fig. 1). It was in operation since the early 18th century up to the late 1980s. In the early 20th century, it became the 1st French coal producer (4.9 million tons/year in 1918; Barau, 2008). The local economy of the study area was thereby essentially based on this industrial coal mining extraction and led to the setting of over 70 coking and/or gas plants (Fig. 1). Furthermore,

related metallurgy activities, weapon, paper mill, smelting and glass plant industries were very active along the OFC.

### 2.2. Sampling site and sediment collection

Dhivert et al. (2015) sampled a previous core in the Villerest flood-control reservoir in 2010 (VIL2010) in order to determine the historical record of heavy metal contamination. A new core sampled in the same sedimentary reservoir in 2012 (VIL2012), allows us to provide information about recorded PAH contamination. The Villerest flood-control reservoir was built between 1976 and 1983 and is located downstream of the industrial and coal mining district (Fig. 1). Water filling operations occurred step by step between 1983 and 1984, and the dam has been in operation since then. It contains 128 mm<sup>3</sup> of water on average and is 36 km long, with a maximum depth of 60 m close to the dam. Three major flood events occurred over the entire upstream basin since the dam operating phase: in 1996 (972 m<sup>3</sup> s<sup>-1</sup>), in 2003 (1570 m<sup>3</sup> s<sup>-1</sup>) and in 2008 (1490 m<sup>3</sup> s<sup>-1</sup>).

The coring site (45°58'54"N, 4°02'15"E) was located 200 m upstream of the Villerest dam (Fig. 1) in the deepest zone of the reservoir. The VIL2012 core was sampled with a UWITEC gravity corer fitted with a 2-m-long and 90-mm-diameter plastic liner. Then, the 130-cm-long core was opened and described. The sampling resolution for organic analysis was chosen according to visual sedimentary description, with a layer thickness ranging from 2 to 6 cm. Overall, 26 slices were freeze-dried and crushed to homogenize prior to analysis.

In addition, some PAHs data is available from the Loire Bretagne Water Agency (LB Agency). In the study area, the LB Agency surveys the sediment quality of 19 stations over the 2005–2010 period and under the European Water Framework (Fig. 1 and Table 1). Bed sediments (0–5 cm) were collected in glass bottles, kept cold (5 °C) and transported to the CARSO laboratory (Lyon, France; [www.groupecarso.com](http://www.groupecarso.com)) for PAH analysis. PAHs concentration ranges of this survey could strengthen our spatial distribution substudy of organic contaminants in ULB sediments around our focused sediment core study.

### 2.3. Analytical protocol

#### 2.3.1. Grain size analysis

Particle size analysis was performed after a 1-min sonication step with a Malvern Mastersizer 3000 laser diffraction microgranulometer on each fresh 2-cm core slice (measurement range between 0.05 and 2000 μm). Grain-size median (D<sub>50</sub>) and cumulative volumetric percentages of clay (<2 μm), silt (<63 μm) and sand (>63 μm) were computed with the Gradistat spreadsheet (Blott and Pye, 2001) using the Folk and Ward geometric method (Folk and Ward, 1957).

#### 2.3.2. PAH analysis

PAHs were extracted using the pressurized liquid extraction (PLE) technique with an accelerated solvent extractor (ASE™ 350, ThermoScientific®). Extraction cells of 34 mL were used and filled with a mixture of 2.5 g of the sediment sample and diatomaceous earth (Sigma Aldrich®). Extractions were carried out with dichloromethane at 100 °C and 100 bars, 5 static cycles of 4 min and a rinse volume of 60%. Extracts were evaporated until dryness under a gentle stream of nitrogen and then reconstituted in 1 mL of dichloromethane. Benzo(a)pyrene D-12 (Sigma–Aldrich®) was then added to the samples as an internal standard. External calibration was performed with a commercial mixture of the 16 PAHs (at 2000 μg/mL each in dichloromethane, Restek®) and a calibration curve (8 standards, 0–250 ng/mL of each compound in

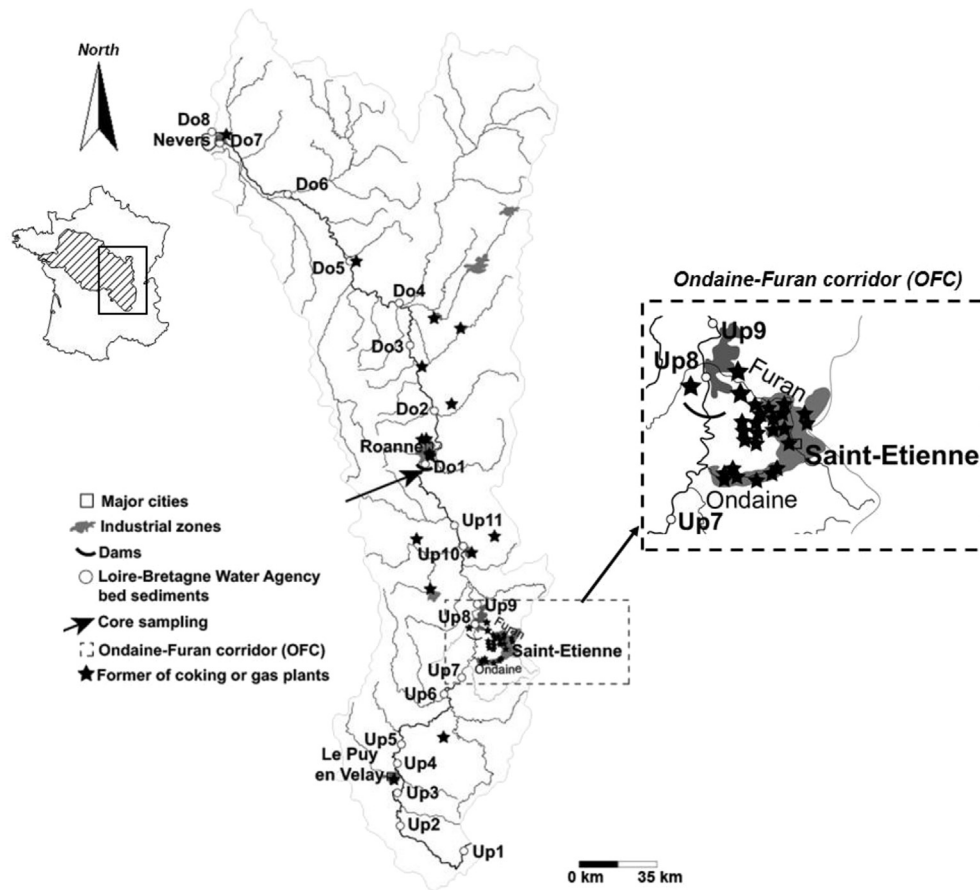


**Fig. 1.** Map of the ULB and the Ondaine-Furan corridor (OFC). The Grangent and Villerest dams are indicated by black half circles. Industrial zones were marked in gray, and black stars represent the locations of former coking or gas plants (data from BaSOL; <http://basol.developpement-durable.gouv.fr/>). The coring site is noted by the black arrow. The sampling points of bed sediments survey by the Loire Bretagne Water Agency (LB Agency) and located upstream (Up) or downstream (Do) of the Villerest flood control reservoir are noted by white circles.

dichloromethane) was realized. Linearity of the calibration curves for individual PAHs were confirmed by the  $r^2$  values (0.905–0.997 range).

The 16 PAHs recommended by U.S. EPA were chosen for investigation: naphthalene (NAP), acenaphthylene (ACY), acenaphthene

(ACE), fluorine (FLU), phenanthrene (PHE), anthracene (ANT), fluoranthene (FLT), pyrene (PYR), benzo(a)anthracene (BaA), chrysene (CHY), benzo(b)fluoranthene (BbF), benzo(k)fluoranthene (BkF), benzo(a)pyrene (BaP), indeno(1,2,3-cd)pyrene (IcdP), dibenzo(ah)anthracene (dBahA) and benzo(ghi)perylene (BghiPL). They were

**Table 1**

General characteristics and number of samples (n) collected at the 19 stations by the Loire-Bretagne Water Agency (LB Agency) and over the 2005–2010 period. Stations are located upstream (Up) or downstream (Do) of the Villerest dam according to their kilometric point (Kp, with Kp = 0 km is the estuary of the Loire river).

| Sampling point | Name                     | n | Kp   | Y (longitude) | X (latitude) |
|----------------|--------------------------|---|------|---------------|--------------|
| Up1            | Sainte-Eulalie           | 3 | 1001 | 44°49'25"N    | 4°11'41"E    |
| Up2            | Goudet                   | 4 | 957  | 44°53'30"N    | 3°55'18"E    |
| Up3            | Coubon                   | 2 | 932  | 44°59'53"N    | 3°55'03"E    |
| Up4            | Le Puy-en-Velay          | 2 | 919  | 45°04'42"N    | 3°54'43"E    |
| Up5            | Saint-Vincent            | 2 | 903  | 45°09'44"N    | 3°55'51"E    |
| Up6            | Bas-en-Basset            | 2 | 861  | 45°17'44"N    | 4°07'06"E    |
| Up7            | Malvalette               | 2 | 854  | 45°19'50"N    | 4°09'15"E    |
| Up8            | Saint-Just-Saint-Rambert | 2 | 823  | 45°30'11"N    | 4°15'33"E    |
| Up9            | Veauchette               | 6 | 814  | 45°33'46"N    | 4°16'19"E    |
| Up10           | Feurs                    | 5 | 788  | 45°44'33"N    | 4°12'44"E    |
| Up11           | Balbigny                 | 5 | 777  | 45°48'55"N    | 4°10'16"E    |
| Do1            | Villerest                | 2 | 741  | 45°59'44"N    | 4°02'49"E    |
| Do2            | Briennon                 | 6 | 719  | 46°08'48"N    | 4°05'52"E    |
| Do3            | Luneau                   | 4 | 689  | 46°21'28"N    | 4°06'08"E    |
| Do4            | La Motte Saint-Jean      | 2 | 664  | 46°29'31"N    | 3°56'28"E    |
| Do5            | Bourbon-Lancy            | 2 | 628  | 46°37'51"N    | 3°43'05"E    |
| Do6            | Decize                   | 4 | 588  | 46°49'41"N    | 3°27'30"E    |
| Do7            | Nevers                   | 5 | 552  | 46°58'57"N    | 3°09'09"E    |
| Do8            | Fourchambault            | 4 | 539  | 47°00'48"N    | 3°04'23"E    |

analyzed by gas chromatography–mass spectrometry (GC–MS). The apparatus was equipped with an automated sampler (Agilent 6890 series, Agilent®). Injections of 1  $\mu\text{L}$  of sample in the injector were performed (splitless, 300 °C). The chromatographic separation was performed on a fused silica capillary Rxi®-XLB column (low polarity, 30 m  $\times$  0.25 mm ID  $\times$  0.25  $\mu\text{m}$ , Restek®) in a GC HP 6890 series (Hewlett Packard, Agilent®). The GC temperature program was: hold 40 °C for 2 min, then 40 °C–240 °C at a rate of 30 °C/min, hold for 2 min, followed by a rate of 10 °C/min until 340 °C, then hold 5 for minutes. Identification was performed by a mass spectrometer (HP 5973, Hewlett Packard, Agilent®). Selective Ion Monitoring (SIM) was chosen for enhancing the quality of the detection. The MSD ChemStation software (Agilent®) was used to control the equipment as well as for the data exploitation.

The extraction rate of the method was determined by replicate analysis ( $n = 13$ ) of a certified reference sediment (CNS391, Sigma Aldrich). The comparison to the certified PAH values indicated that our method recovered between 41% and 105% of almost all compounds, excepted for NAP, ACE, FLU (for these compounds extraction yield were about 20%). The detection limits (LOD) and the quantification limits (LOQ) were determined as a signal to noise ratio of 3 and 10 (blank analysis,  $n = 10$ ) and ranged from 3 to 7  $\mu\text{g}/\text{kg}$  and 6–17  $\mu\text{g}/\text{kg}$ , respectively. Periodic quality control consisted of analyses of blanks and certified reference materials (CNS391, Sigma Aldrich).

For bed sediment survey carried by the LB Agency, the CARSO laboratory did PAH analyses on freeze-dried and sieved (<2 mm) samples. The extractable organic matter was extracted by a hexane/acetone mixture using an automated extractor and the 16 priority PAHs were analyzed using high-performance liquid chromatography with postcolumn fluorescence derivatization (HPLC/FLD). Comparability of the GC/MS method used in this work and the HPLC/FLD method used by the CARSO laboratory was evaluated by the analysis of the certified reference sediment (CNS391, Sigma Aldrich). Extraction yields are in the 41–105% range (excepted NAP, ACE, FLU: 20%) and in the 28–94% range (excepted NAP, ACE, FLU:

20%) for the GC/MS method and for the HPLC/FLD method respectively.

### 3. Results and discussion

#### 3.1. Sedimentological description and evidence of flood events

The sedimentological description of the VIL2012 core is presented in Fig. 2a. Two sedimentary units have been highlighted based on the comparison of the percentage of clays of our studied core VIL2012 with the core VIL2010, presented in Dhivert et al. (2015; Fig. 2b). These latter authors determined the Cs-based model age and hydrological conditions of sediments deposited in VIL2010 using sedimentological and geochemical markers. Considering the sedimentary similarities of the two cores, the same hydrological interpretations can be achieved with VIL2012.

Unit 2 (U2) is constant in color and texture and includes fine-grained sands between 130 and 83 cm (Fig. 2a). The percentages of sand, silt and clay range from 12 to 55%, 42–80% and approximately 5% (Fig. 2b), respectively. Sediments correspond to a mix between decantation in lentic environment and the fluvial domain. They may have been deposited, reworked and winnowed during the dam construction (1976–1983) and reservoir water filling (1983–1984). Unit 1 (U1) corresponds to sediments above 83 cm. A slight decrease in the percentage of sand (ranging from 28 to 4%), and conversely an increase in the percentage of silt, (ranging from 66 to 86%) can be observed. The percentage of clay ranges from 4 to 8% (Fig. 2b). Sediments of U1 were settled by decantation under lacustrine conditions as they exist in the flood-control reservoir. Moreover, this unit is also well laminated with alternating fine and darker bands. Conversely, well defined coarser and lighter layers occurred at 60–54 cm, at 44–32 cm and at 22–10 cm (gray stripes; Fig. 2a and b). Dhivert et al. (2015) demonstrated that these layers recorded in VIL2010 correspond to major floods that occurred since the dam operating phase, i.e., the 1996, 2003 and 2008 floods. The percentage of clay in these three particular layer

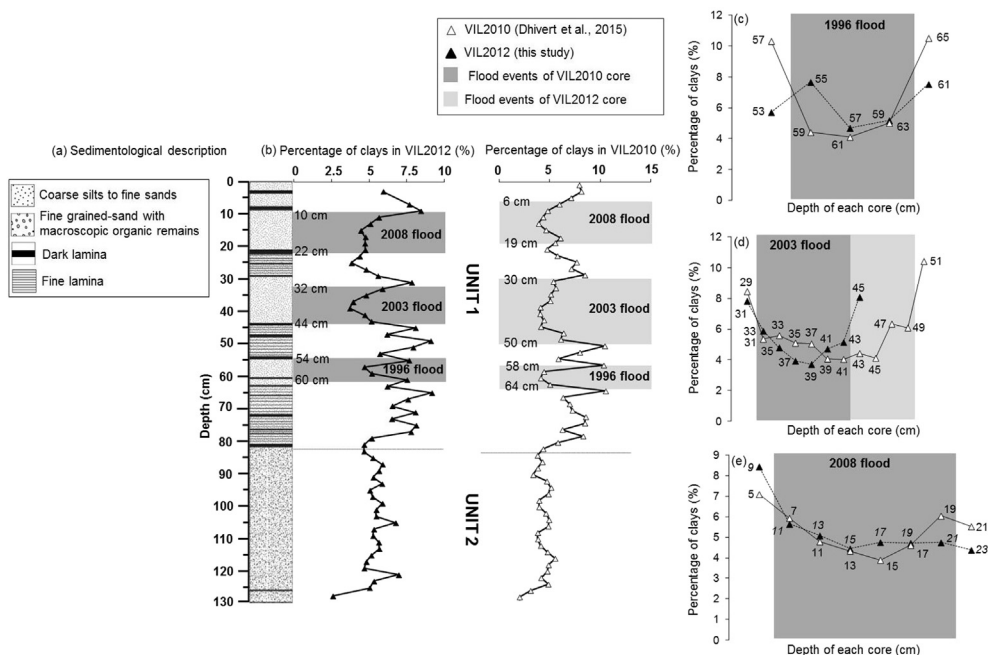


**Fig. 2.** (a) Sedimentological description of the VIL2012 core; (b) Percentage of clays (<4  $\mu\text{m}$ ) in VIL2010 (white triangles) and VIL2012 (dark triangles) cores. The three major flood events (1996, 2003 and 2008) are marked by light gray (VIL2010) and dark gray (VIL2012) rectangles. Comparison of the clay percentage profile in each sample, including coarser and lighter layers, are presented for the 1996 (c), 2003 (d) and 2008 (e) flood sequences in VIL2010 (light gray triangles) and VIL2012 cores (dark gray triangles). Numbers correspond to the mean depth of 2 cm core slices.

**Table 2**

Concentrations of the 2–3 rings ( $\Sigma 2\text{-}3\text{-rings}$ ), 4-rings ( $\Sigma 4\text{-rings}$ ) and 5–6-rings ( $\Sigma 5\text{-}6\text{-rings}$ ) PAHs and of the sum of the priority PAHs ( $\Sigma 16\text{PAHs}$ ) for VIL2012 core. Samples were separated according to unit 1 (U1) and 2 (U2). Samples recorded the three major floods events (1996, 2003 and 2008) are marked by dark gray rectangles. Pollution levels were established from  $\Sigma 16\text{PAHs}$  as low = 0–100 ng/g; moderate >100–1000 ng/g; high >1000–5000 ng/g; very high >5000 ng/g, according to Baumard et al., 1998.

|      | Depth (cm) | $\Sigma 2\text{-}3\text{-rings}$ | $\Sigma 4\text{-rings}$ | $\Sigma 5\text{-}6\text{-rings}$ | $\Sigma 16\text{PAHs}$ | Pollution level (Baumard et al., 1998) |
|------|------------|----------------------------------|-------------------------|----------------------------------|------------------------|--|
| U1   | 1.5        | 738                              | 1410                    | 3648                             | 5795                   | Very high                              |
|      | 4          | 298                              | 679                     | 869                              | 1846                   | High                                   |
|      | 6          | 281                              | 830                     | 866                              | 1977                   | High                                   |
|      | 8.5        | 215                              | 822                     | 3615                             | 4652                   | High                                   |
|      | 12.5       | 390                              | 1138                    | 1393                             | 2921                   | High                                   |
|      | 17.5       | 474                              | 1562                    | 3446                             | 5482                   | Very high                              |
|      | 22.5       | 321                              | 910                     | 4846                             | 6077                   | Very high                              |
|      | 27.5       | 334                              | 1132                    | 2486                             | 3951                   | High                                   |
|      | 34         | 560                              | 1703                    | 4000                             | 5362                   | Very high                              |
|      | 40.5       | 242                              | 1105                    | 1883                             | 3230                   | High                                   |
|      | 44.5       | 332                              | 1073                    | 1294                             | 2699                   | High                                   |
|      | 47.5       | 153                              | 711                     | 865                              | 1729                   | High                                   |
|      | 51.5       | 289                              | 1020                    | 2068                             | 3377                   | High                                   |
|      | 58         | 466                              | 1120                    | 4796                             | 6382                   | Very high                              |
|      | 64.5       | 215                              | 820                     | 1071                             | 2106                   | High                                   |
|      | 67.5       | 327                              | 1256                    | 3026                             | 4609                   | High                                   |
|      | 70         | 277                              | 1016                    | 1319                             | 2612                   | High                                   |
| 75   | 263        | 1119                             | 1410                    | 2792                             | High                   |  |
| 80.5 | 653        | 2323                             | 9010                    | 11986                            | Very high              |  |
| U2   | 84.5       | 1009                             | 4292                    | 8048                             | 13349                  | Very high                              |
|      | 88         | 479                              | 2124                    | 2316                             | 4919                   | High                                   |
|      | 98         | 804                              | 1917                    | 2091                             | 4811                   | High                                   |
|      | 106        | 1075                             | 2436                    | 2263                             | 5774                   | Very high                              |
|      | 113        | 802                              | 3039                    | 5686                             | 9527                   | Very high                              |
|      | 122        | 586                              | 2003                    | 2294                             | 4883                   | High                                   |
|      | 128.5      | 270                              | 1483                    | 2676                             | 4429                   | High                                   |

assemblages allows us to clearly confirm the top and the bottom of the flood sequences in VIL2012 (Fig. 2c, d and e). Indeed, considering each flood event, the pattern in the percentage of clay are similar in the two cores even if the depths are slightly shifted. More specifically, the 1996, 2003 and 2008 flood sequences are recorded between 60 and 54 cm (Fig. 2b and c), 44–32 cm (Fig. 2b and d) and 22–10 cm (Fig. 2b and e) in the VIL2012 core.

### 3.2. Historical chronicles of PAHs contamination

#### 3.2.1. Temporal evolution and contamination level of PAHs

On the basis of the number of aromatic rings, PAHs can be classified between low molecular weight PAHs (2–3 rings), which are major components of crude oil and its refined products and medium and high molecular weight PAHs (4-rings and 5–6 rings respectively), mainly generated by high temperature combustion

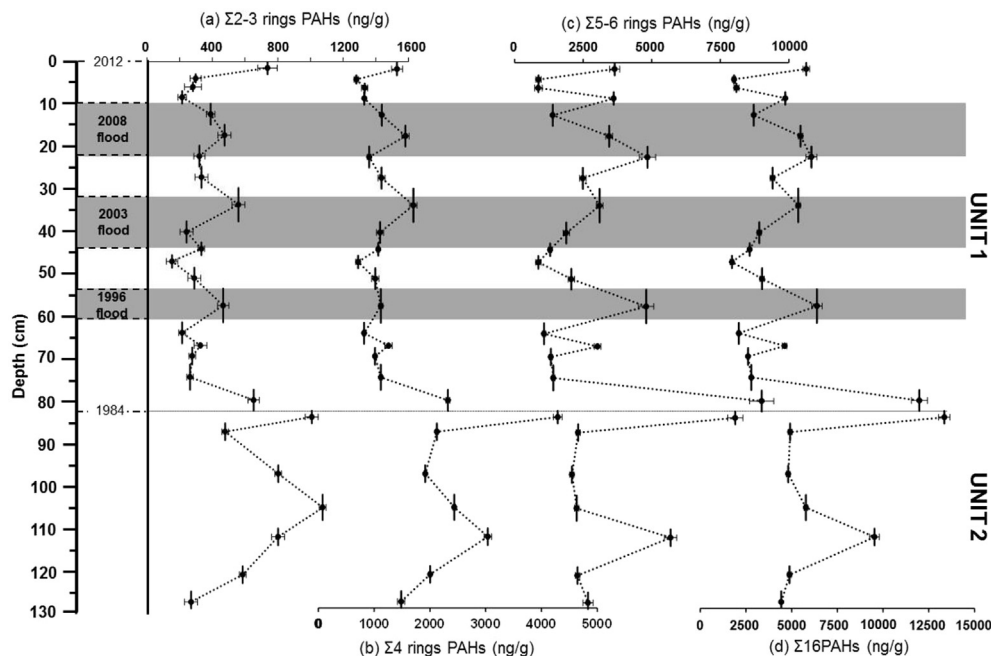


**Fig. 3.** Concentrations (ng/g) of (a)  $\Sigma 2\text{-}3$  rings, (b)  $\Sigma 4$  rings and (c)  $\Sigma 5\text{-}6$  rings PAHs and (d)  $\Sigma 16\text{PAHs}$  (ng/g) vs. depth (cm). The vertical lines represent the thickness of each sample, whereas the horizontal lines represent the analytical uncertainties of each measurement. The three major flood events (1996, 2003 and 2008) are marked by dark gray rectangles.

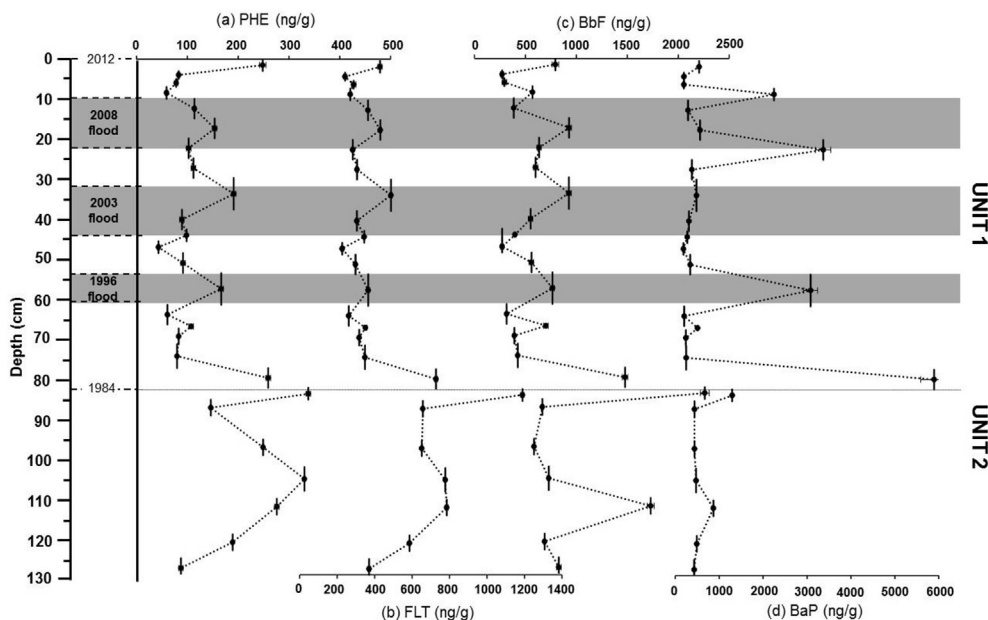


**Fig. 4.** Concentrations (ng/g) of (a) phenanthrene (PHE), (b) floranthene (FLT) (c) benzo(b)fluoranthene (BbF) and (d) benzo(a)pyrene (BaP) vs. depth (cm). The vertical lines represent the thickness of each sample, whereas the horizontal lines represent the analytical uncertainties of each measurement. The three major flood events (1996, 2003 and 2008) are marked by dark gray rectangles.

(Fernandes et al., 1999; Meyers and Ishiwatari, 1993; Yunker and Macdonald, 2003). Table 2 and Fig. 3 illustrate concentrations of the low ( $\Sigma 2$ -3-rings), medium ( $\Sigma 4$ -rings) and high molecular weight PAHs ( $\Sigma 5$ -6 rings) and of the sum of the 16 priority PAHs ( $\Sigma 16$ PAHs) in the VIL2012 sediment core (ng/g of dry sediment).  $\Sigma 16$ PAHs is relatively high and varied from 1729 ng/g at 47.5 cm up to 13,349 ng/g at 84.5 cm. Baumard et al. (1998) classified Mediterranean Sea sediments with four pollution levels: lowly ( $\Sigma$ PAHs = 0–100 ng/g), moderately ( $\Sigma$ PAHs > 100–1000 ng/g), highly ( $\Sigma$ PAHs > 1000–5000 ng/g) and very highly contaminated ( $\Sigma$ PAHs > 5000 ng/g). These same pollution levels were used for  $\Sigma 16$ PAHs. This pollution levels classification reveals that VIL2012 core samples could be classified as highly to very highly contaminated sediments. The oldest U2, which are deposited prior 1984, includes most contaminated sediments (ranging from 4428 to 13348 ng/g; Table 2 and Fig. 3d). The highest concentrations of  $\Sigma 16$ PAHs are present at 113 cm (9527 ng/g) and at the very top of U2 (84.5 cm: 13349 ng/g). This latter increase could correspond to the end of the reservoir water filling operations occurring between 1983 and 1984. The most recent sediments deposited after 1984 were included in U1. Six  $\Sigma 16$ PAHs peaks are observed at 80.5 cm (11,986 ng/g), 67.5 cm (4609 ng/g), 58 cm (6382 ng/g), 34 cm (5362 ng/g), 22.5 cm (6077 ng/g) and 8.5 cm (4652 ng/g; Table 2 and Fig. 3d). Three of six increases correspond to flood periods (58 cm: 1996-flood, 34 cm: 2003-flood and 22.5 cm: 2008-flood; Fig. 3). It could be attributed to specific sources appearing during these particular hydrological conditions and/or to a grain-size effect also pointed out in Rhône river PCB sediment record (Desmet et al., 2012; Mourier et al., 2014). These peaks are characterized by very highly contaminated sediments (Table 2). Finally, an increase in  $\Sigma 16$ PAHs can also be observed at the water-sediment interface (5795 ng/g; Table 2 and Fig. 3d).

Low molecular weight PAHs ( $\Sigma 2$ -3-rings) represent a maximum of 20% of  $\Sigma 16$ PAHs. The major 2-3-rings PAH was PHE, which represents about 6% of  $\Sigma 16$ PAHs. More accurately, highest concentration of PHE are recorded in the oldest sediments of U2 (at 106 cm: 661 ng/g and 84.5 cm: 676 ng/g; Fig. 4a) and reached 11% of

$\Sigma 16$ PAHs. This latter compound is considered as potential chemical tracer for vehicle emissions (Harrison et al., 1996; Simcik et al., 1999). Thus, the high values of PHE and consequently of 2-3-rings PAHs could be explained by the use of motor vehicles during the dam construction. In contrast, medium and high molecular weight PAHs represent 15–43% (ranging from 679 to 4292 ng/g) and 39–80% (ranging from 865 to 9010 ng/g) of  $\Sigma 16$ PAHs respectively (Table 2; Fig. 3b and c). Among 4-rings PAHs, FLT represents about 10% of  $\Sigma 16$ PAHs, following by PYR (ca. 8%), CHY (ca. 7%) and BaA (ca. 7%). The highest concentrations of FLT are recorded at 113 cm (785 ng/g) and during the end of the water filling operations (84.5: 1189 ng/g; Fig. 4b). In U1, five peaks are observed at 80.5 cm (728 ng/g), 58 cm (365 ng/g), 34 cm (487 ng/g) and 22.5 cm (430 ng/g) and at the water-sediment interface (429 ng/g; Fig. 4b). The same trends are observed for the concentration of other 4-rings PAHs, such as PYR, BaA and CHY. Finally, among 5-6-rings PAHs, BbF (ca. 15%), BaP (ca. 16%), dBahA (ca. 10%) and BghiPL (ca. 9%) were prevalent in most of the samples. The evolution of 5-6 rings PAHs, such as BbF, follows the variations of 4-rings PAHs (Fig. 3c) even if two other increasing are recorded (at 67.5 cm: 701 ng/g and at 8.5 cm: 571 ng/g; Fig. 4c). Furthermore, in 4 core levels of U1, BaP becomes the predominant PAH, representing 48–55% of  $\Sigma 16$ PAHs (5895 ng/kg at 80.5 cm; 3082 ng/kg at 58 cm; 3367 ng/kg at 22.5 cm and 2250 ng/kg at 8.5 cm; Fig. 4d). This compound has been investigated as a marker for some combustion-derived PAHs since its concentration in petroleum is usually negligible (Magi et al., 2002).

### 3.2.2. Regional and international environmental implications

For greater perspective, we compare the registered levels in VIL2012 to longitudinal variations of  $\Sigma 16$ PAHs in the broader context of the ULB. Table 3 provides minimum, maximum values and sum of median concentrations of the 2-3-rings, 4-rings, 5-6 rings PAHs and 16 priority PAHs (ng/g of dry sediment) for 19 stations collected by the LB Agency over the period 2005–2010. The bed sediment dataset indicates that  $\Sigma 16$ PAHs range from 394 to 7460 ng/g (Table 3). These level ranges are in good agreement with

**Table 3**

Minimum, maximum values, sum of the median concentrations and quantification limits (ng/g) of 2–3 rings ( $\Sigma$ 2–3-rings), 4-rings ( $\Sigma$ 4-rings) and 5–6-rings ( $\Sigma$  5–6 rings) PAHs and of the sum of the 16 priority PAHs ( $\Sigma$ 16PAHs), for the 19 stations sampled by the Loire-Bretagne Water Agency (LB Agency) over the 2005–2010 period. Pollution levels of bed sediments were established from the sum of the median values of  $\Sigma$ 16PAHs as low = 0–100 ng/g; moderate >100–1000 ng/g; high >1000–5000 ng/g; very high >5000 ng/g, according to Baumard et al., 1998.

|      | $\Sigma$ 2-3-rings |      |        | $\Sigma$ 4-rings |      |        | $\Sigma$ 5-6 rings |      |        | $\Sigma$ 16PAHs |       |        | Pollution level<br>(Baumard et al., 1998) |
|------|--------------------|------|--------|------------------|------|--------|--------------------|------|--------|-----------------|-------|--------|---|
|      | Min                | Max  | Median | Min              | Max  | Median | Min                | Max  | Median | Min             | Max   | Median |   |
| Up1  | 128                | 150  | 145    | 100              | 356  | 235    | 96                 | 419  | 181    | 346             | 903   | 561    | Moderate                                  |
| Up2  | 75                 | 244  | 105    | 120              | 948  | 256    | 119                | 676  | 234    | 364             | 1868  | 569    | Moderate                                  |
| Up3  | 150                | 152  | 151    | 100              | 342  | 221    | 100                | 316  | 208    | 350             | 810   | 580    | Moderate                                  |
| Up4  | 159                | 408  | 2834   | 654              | 2135 | 1395   | 524                | 1440 | 982    | 1337            | 3983  | 2660   | High                                      |
| Up5  | 192                | 476  | 334    | 648              | 1054 | 851    | 599                | 632  | 616    | 1472            | 2129  | 1801   | High                                      |
| Up6  | 161                | 186  | 174    | 834              | 901  | 868    | 761                | 786  | 774    | 1781            | 1848  | 1815   | High                                      |
| Up7  | 137                | 195  | 166    | 196              | 647  | 422    | 222                | 574  | 398    | 555             | 1416  | 985,5  | Moderate                                  |
| Up8  | 203                | 313  | 258    | 797              | 870  | 834    | 571                | 590  | 581    | 1590            | 1754  | 1672   | High                                      |
| Up9  | 629                | 2013 | 1882   | 974              | 5097 | 3323   | 927                | 3805 | 2255   | 2530            | 10869 | 7460   | Very high                                 |
| Up10 | 256                | 1847 | 661    | 509              | 3070 | 1612   | 585                | 2723 | 1510   | 1350            | 7640  | 3783   | High                                      |
| Up11 | 270                | 1306 | 345    | 488              | 2603 | 962    | 535                | 1514 | 857    | 1445            | 5423  | 2264   | High                                      |
| Do1  | 353                | 506  | 430    | 921              | 2484 | 1703   | 718                | 2154 | 1436   | 1992            | 5144  | 3568   | High                                      |
| Do2  | 137                | 340  | 254    | 286              | 1233 | 627    | 394                | 738  | 539    | 861             | 2311  | 1416   | High                                      |
| Do3  | 93                 | 369  | 147    | 148              | 957  | 233    | 144                | 715  | 242    | 385             | 2041  | 622    | Moderate                                  |
| Do4  | 287                | 511  | 399    | 1117             | 1375 | 1246   | 674                | 1192 | 933    | 2078            | 3078  | 2578   | High                                      |
| Do5  | 125                | 125  | 125    | 100              | 100  | 100    | 98                 | 239  | 169    | 323             | 464   | 394    | Moderate                                  |
| Do6  | 60                 | 581  | 191    | 40               | 1227 | 375    | 60                 | 1167 | 335    | 160             | 2975  | 900    | Moderate                                  |
| Do7  | 68                 | 451  | 288    | 40               | 1060 | 609    | 60                 | 1160 | 545    | 168             | 2518  | 1605   | High                                      |
| Do8  | 69                 | 179  | 126    | 70               | 401  | 175    | 78                 | 301  | 159    | 217             | 881   | 459    | Moderate                                  |
| QL   | 60                 | 60   | 60     | 40               | 40   | 40     | 52                 | 52   | 52     | 152             | 152   | 152    |   |

the ones registered in U1 of VIL2012 (1729 up to 6382 ng/g; Table 2). Specifically, medium and high molecular weight PAHs were the most frequently detected PAHs in the VIL2012 core samples as well as in ULB bed sediments. Their median concentrations

ranged between 100 and 3323 ng/g and 159 and 2255 ng/g, averaging 43 and 38% of  $\Sigma$ 16PAHs respectively.

At the ULB scale, the lowest PAHs levels are observed in the most upstream and downstream parts (sites upstream the OFC, Up1 to

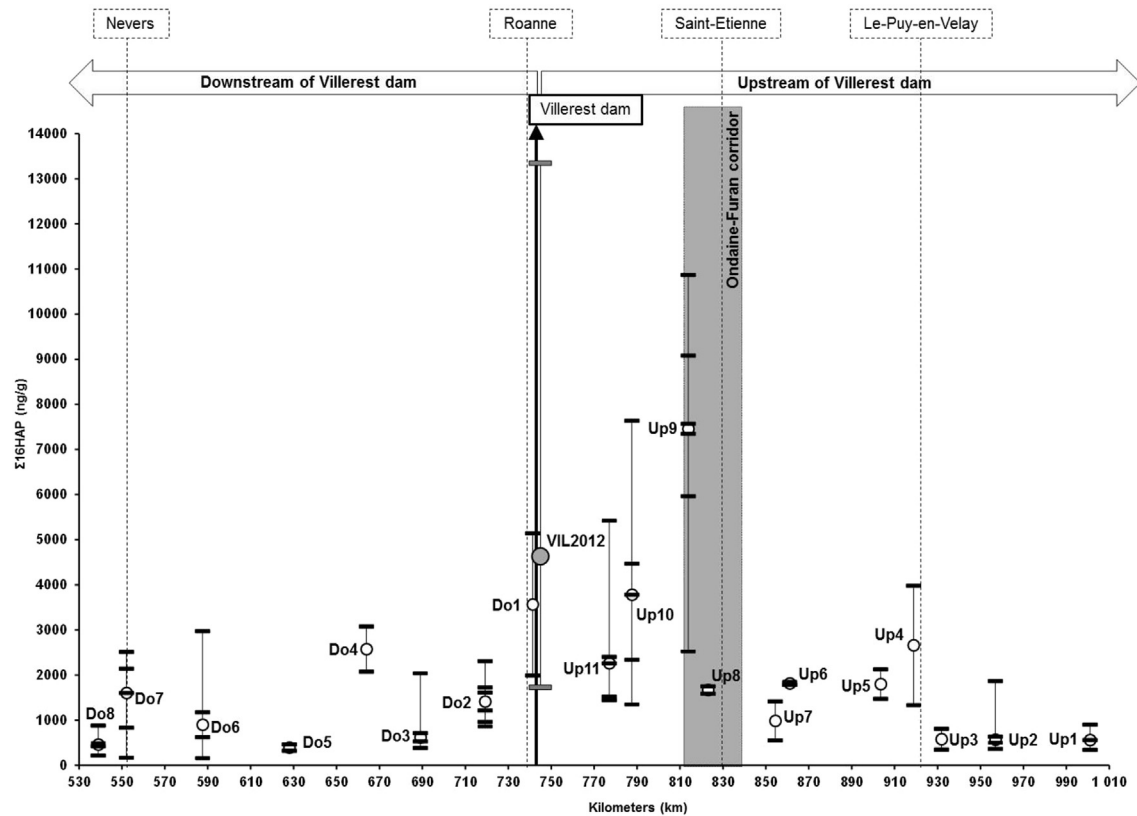


**Fig. 5.** Longitudinal profile (kilometers point) of  $\Sigma$ 16PAHs (ng/g) in Upper Loire Basin (ULB) bed sediments. White circles represent the sum of the median concentrations of the 16 priority PAHs over the period 2005–2010. Dark dash represents each sampled year value. The reported maximum, minimum and mean concentrations of the VIL2012 core sediment are noted in gray.

Up7; ranging from 561 to 2660 ng/g; sites downstream the OFC, Do2 to Do8; ranging from 394 to 2578 ng/g; Table 3; Fig. 5). The obtained data are in good agreement with those reported in the literature for other French aquatic systems such as the Garonne and Dordogne rivers ( $\Sigma$ PAHs ranged from 949 to 1566 ng/g and 882–1930, respectively; Budzinski et al., 1997) which are considered moderately polluted by PAHs (Baumard et al., 1998). Moreover, downstream of the OFC (site Up8 to Do1), the  $\Sigma$ 16PAHs concentrations are the highest (ranging from 2264 to 7460 ng/g) over 80 km (Fig. 5). The VIL2012 top-core sediment sample (0–3 cm; 5795 ng/g) is characterized by the same magnitude of  $\Sigma$ 16PAHs concentrations (Fig. 5). Medium and high molecular weight PAHs were prevalent, which represent between 43 and 48% (834–3323 ng/g) and 31–40% (581–2255 ng/g) of  $\Sigma$ 16PAHs respectively. Thus, this bed sediments section can be considered highly to very highly contaminated (2264–7460 ng/g; Table 3; Baumard et al., 1998) which is consistent with the pollution levels defined in VIL2012 (Table 2).

The highest  $\Sigma$ 16PAHs level are observed in site Up9 (maximum of 10,869 ng/g; Table 3) and at 84.5 cm in VIL2012 (13,349 ng/g; Table 2). These concentrations reached the average value recorded in another highly contaminated French basin (Seine River, 10,900 ng/g Carpentier et al., 2002). In other industrialized countries, the inventories of PAHs in bed sediments showed similar results in the Susquehanna River (1547–9847 ng/g; Ko et al., 2007) and in the San Francisco Bay (2944–29,590; Pereira et al., 1996). Nevertheless, results from ULB sediments were much lower than those measured in other highly contaminated river sediments from coal districts (Li et al., 1998; Gu et al., 2003; Christensen and Bzdusek, 2005). For example, Li et al., 1998 investigated seven cores sampled in the Kinnickinnic River, close to the former Wisconsin Solvay Coke Company. In this study area, the highest  $\Sigma$ 16PAHs range from 3,60,000 to 11,00,000 ng/g.

### 3.2.3. Potential toxicity of PAHs

Some PAHs are a great concern due to their carcinogenic effects. In VIL2012 samples, total concentrations of potentially carcinogenic PAHs ( $\Sigma$ CPAHs), including BaA, BbF, BkF, BaP, IcdP and dBahA (Savinov et al., 2003) varied from 831 to 9040 ng/g and accounted

for 44–79% of  $\Sigma$ 16PAHs.  $\Sigma$ CPAHs values were much higher than those measured in bed sediment survey downstream of the OFC (ranging from 414 to 1962 ng/g and accounted for 26–33% of  $\Sigma$ 16PAHs). One approach for estimating the carcinogenic potency associated with the exposure to BaP and other PAHs relative to BaP can be obtained by calculating the total toxic BaP-equivalent (TEQ<sub>carc</sub>, Qiao et al., 2006):

$$TEQ^{carc} = \sum_i C_i \times TEF_i^{carc} \quad (1)$$

where, C is the concentration of BaA, BbF, BkF, BaP, IcdP and dBahA and  $TEF_i^{carc}$  is their associated equivalent factor (0.1, 1, 0.1, 0.01, 0.1 and 1, respectively; Peters et al., 1999; Qiao et al., 2006).

TEQ<sub>carc</sub> values are higher (ranging from 283 to 6290 ngTEQ/g) than those reported in the literature for another heavily industrialized and populated area in the Taihu Lake sediments (China; TEQ<sub>carc</sub> ca. 94–856 ng/g; Qiao et al., 2006). The maximum values of TEQ<sub>carc</sub> are recorded during the end of the reservoir water filling operations (84.5 cm: 6290 ng/TEQ/g), and during the three major flood events, reaching up to 3270, 876 and 3540 ngTEQ/g respectively. These TEQ<sub>carc</sub> values are in the same range than those calculated by García et al. (2012) for highly polluted soil samples, at a distance of about 50 km from the coking battery (Oviedo, Spain; ca. 1040–4080 ng/g).

### 3.3. Source identification of PAHs

#### 3.3.1. PAHs intercorrelation approach

In the VIL2012 core samples, 4-rings and 5-6-rings PAHs were predominant and several typical pyrogenic PAH were present in high concentrations (PHE, FLT, PYR, CHY, BbF, BkF, IcdP, BghiPL; Fernandez et al., 2000). For example, previous studies indicate that FLT is one of the major products during combustion of wood and coal (Li et al., 2006; Masclat et al., 1987). This kind of source could be confirmed by the significant correlation observed between the sedimentary concentrations of two of the predominant 4-rings PAHs (FLT vs. PYR) illustrated in Fig. 6a ( $R^2 > 0.99$ ). FLT and PYR were often associated in natural matrices and were considered as

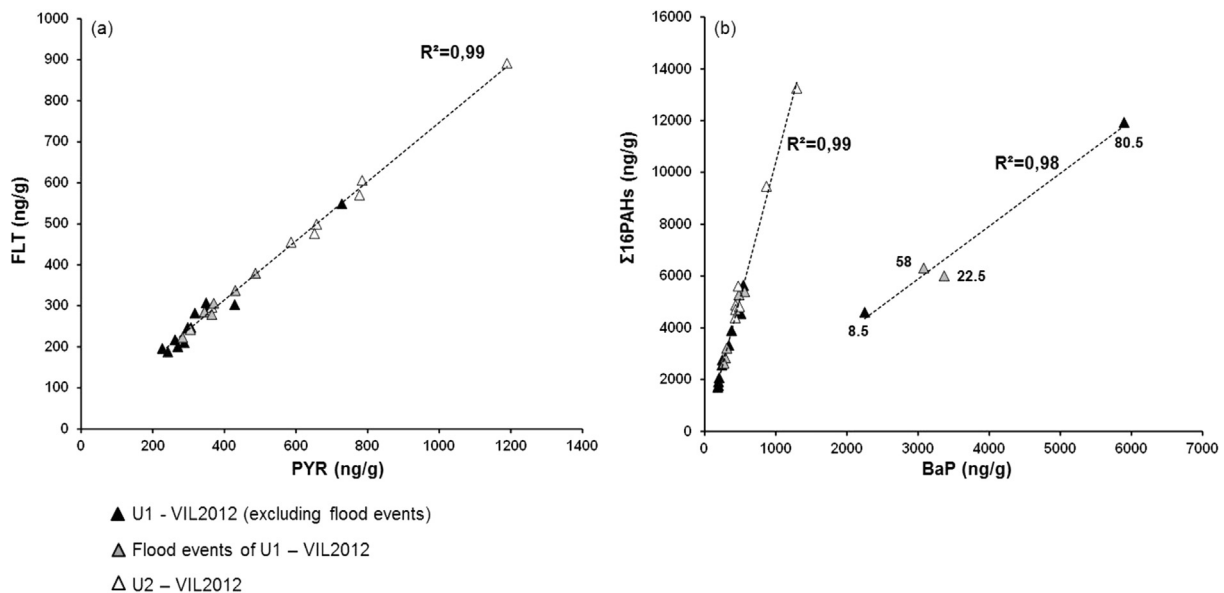
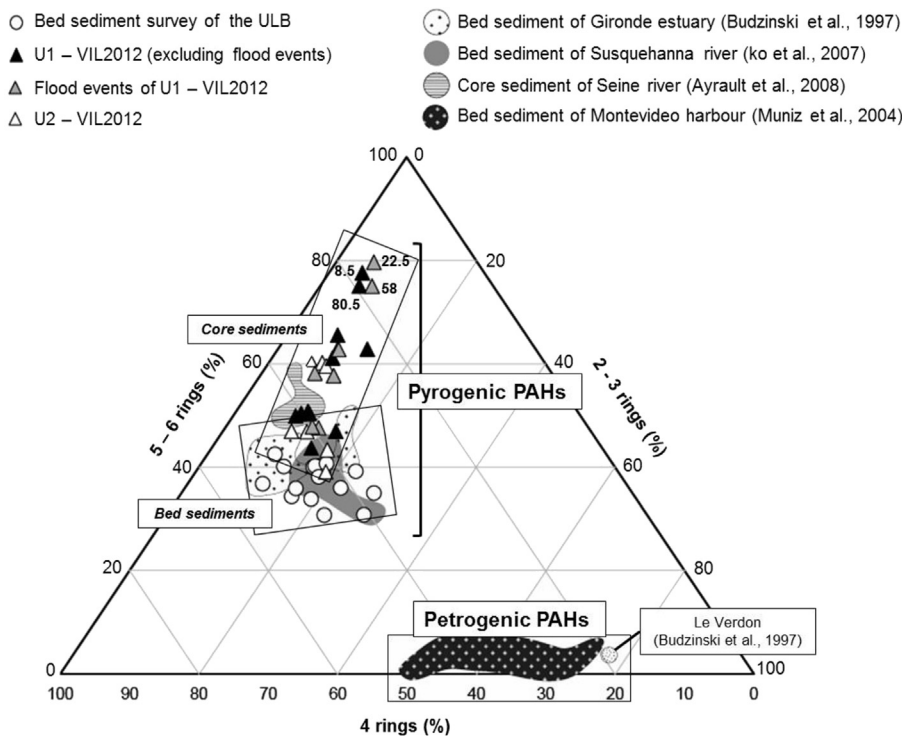


Fig. 6. Significant correlation between concentrations of pyrene (PYR) vs. fluoranthene (FLT) (a) and benzo(a)pyrene (BaP) vs.  $\Sigma$ 16PAHs. Depth levels are associated to specific samples.



**Fig. 7.** Triangular diagram of the proportions of 2-3 ring, 4 ring and 5-6 ring PAHs calculated from the median PAH concentrations in the Upper Loire Basin bed sediments and in VIL2012 core samples. Do5 station is not reported because most of the PAH concentration were below the quantification limit. Depth levels are reported for specific samples.

typical pyrogenic products derived from high-temperature condensation of low molecular weight PAHs (Soclo et al., 2000).

This is validated by using a triangular diagram of percentage concentrations of  $\Sigma 16\text{PAHs}$  (Qiao et al., 2006, Fig. 7). According to the numbers of aromatic rings, the PAH composition of VIL2012

core samples are globally depleted in 2-3-ring PAHs to the benefit of 4-rings (18–44%) and 5-6-ring PAHs (39–78%). This phenomenon was also observed for core sediments sampled in the Seine River (Ayrault et al., 2008; Fig. 7). This can be attributed to PAHs derived from a pyrogenic origin and/or to environmental

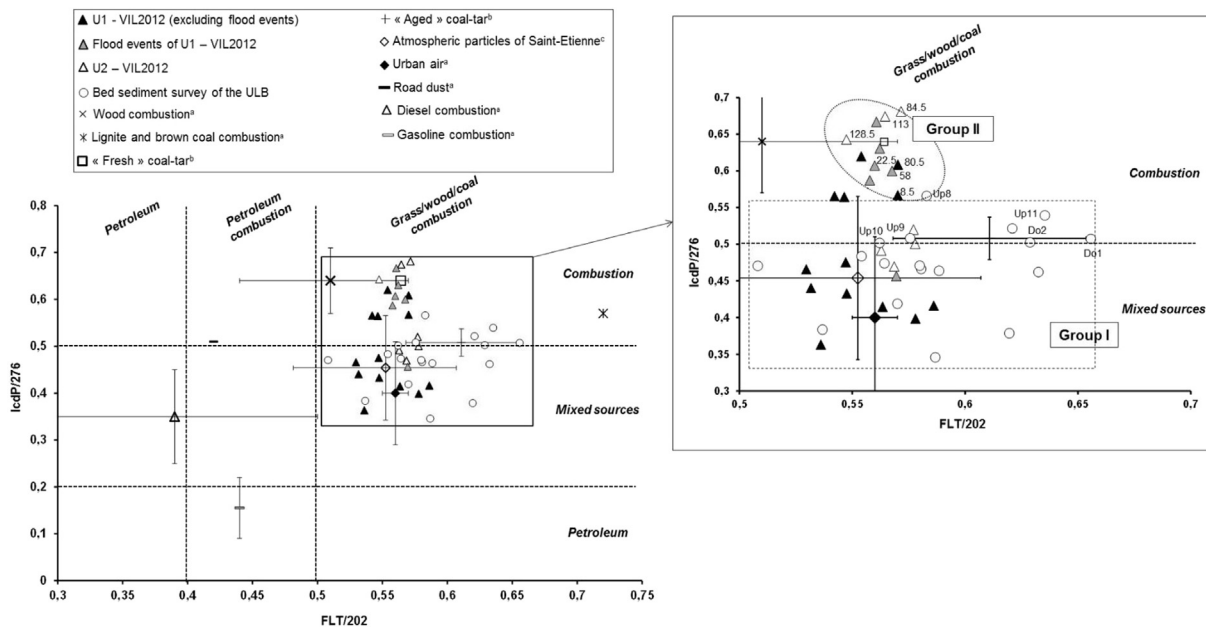


**Fig. 8.** Cross-plot of FLT/202 vs. IcdP/276 for VIL2012 core samples (dark, white and gray triangles) and ULB bed sediments (white circles) and comparison with pure sources determined from the literature (a: Yunker et al., 2002; b: Biache et al., 2014) and from data obtained by Air Rhône-Alpes<sup>®</sup> (www.air-rhonealpes.fr). Do5 station is not reported because FLT, PYR and BghiPL concentration were below the quantification limit. Source boundary lines in this figure are based on Yunker et al. (2002). Depth levels are reported for specific samples.

degradation of 2-3 rings PAHs by oxidation, photo-oxidation processes and/or microbial activity (Fasnacht and Blough, 2002; Hinga, 2003; Rothermich et al., 2002). In contrast, 4-rings and 5-6-rings PAHs are more resistant to degradation (Cerniglia, 1992; Quantin et al., 2005). Moreover, it is specifically interesting to note that the 4 particular samples, which are highly contaminated with BaP (80.5, 58, 22.5 and 8.5 cm), indicating logically a shift towards higher proportions of 5-6-ring PAHs. These results can show a change in the PAHs pyrogenic sources. Indeed, coal combustion could be largely responsible for elevated concentrations of BaP and this compound could be then used as a tracer of coke production (Duval and Friedlander, 1982; Harrison et al., 1996). This is verified by the linear regression between BaP and  $\Sigma 16\text{PAHs}$  in VIL2012 sediments ( $R^2 > 0.99$ ) whereas these 4 particular samples are not included (Fig. 6b). However, they are significantly correlated together ( $R^2 = 0.98$ ). When compared to ULB bed sediment survey, lower proportions of PAH species with 5-6 rings (31–43%) were detected. The distribution of PAHs is close to those documented in bed sediments of other aquatic environments (Fig. 7; Budzinski et al., 1997; Ko et al., 2007). In these studies, the authors concluded a pyrolytic origin for PAHs in sediments except for one station located near the Verdon harbor in the Gironde estuary (Budzinski et al., 1997). These latter station, which is depleted in 4-6-ring PAHs, is close to Montevideo harbor bed sediments and could then reflect a localized strong input of petrogenic material (Muniz et al., 2004).

### 3.3.2. PAH ratios approach

Assessments of PAH diagnostic ratios conventionally reported in the literature have been widely used to infer combustion-derived PAH sources between fuel combustion, coal and wood combustion or atmospheric deposition processes (Yunker et al., 2002). Fig. 8 shows a cross-plot between medium and high molecular weight PAH ratios ( $\text{FLT}/(\text{FLT} + \text{PYR})$ ; FLT/202 and  $\text{IcdP}/(\text{IcdP} + \text{BghiPL})$ ; IcdP/276). Source boundary lines are based on Yunker et al. (2002). A FLT/202 ratio lower than 0.4 suggests typical petroleum contamination, whereas FLT/202 higher than 0.5 indicates that PAHs are mainly derived from combustion of grass, wood and coal.  $0.4 < \text{FLT}/202 < 0.5$  indicates an origin from combustion of petroleum. The assignment of combustion sources has been corroborated by IcdP/276 ratio. IcdP/276 lower than 0.2 indicated petroleum contamination, whereas a ratio higher than 0.5 is consistent with a biomass combustion source. Finally,  $0.4 < \text{IcdP}/276 < 0.5$  is consistent with petroleum combustion.

To complement the diagnostic ratios interpretation and because pyrogenic PAHs can be derived from several high temperature processes in the ULB area, our results have been also compared to actual sources of combustion reported in Yunker et al. (2002). Additional well-defined samples were reported for comparison, the urban/industrial atmosphere of Saint Etienne ([www.air-rhonealpes.fr](http://www.air-rhonealpes.fr)), a “fresh” and an “aged” coal tar sampled in a former coking plant site (Biache et al., 2014). Indeed, it is the major residue generated during high temperature production of coke or gas (Mendonça and Picado, 2002). Then, we chose to report the “aged” coal tar which has been naturally altered through aging process (oxidation, biodegradation, leaching).

Most of the VIL2012 core samples exhibit a ratio of FLT/202 between 0.53 and 0.59 and IcdP/276 ranging of 0.36–0.57 (group I). These values suggest the dominance of mixed sources, especially derived from particles of urban ( $\text{FLT}/202 = 0.56 \pm 0.01$ ;  $\text{IcdP}/276 = 0.4 \pm 0.11$ ) and industrial air of Saint Etienne ( $\text{FLT}/202 = 0.55 \pm 0.06$ ;  $\text{IcdP}/276 = 0.45 \pm 0.11$ ), with some contribution from “aged” coal-tar washout ( $\text{FLT}/202 = 0.61 \pm 0.04$ ;  $\text{IcdP}/276 = 0.51 \pm 0.02$ ). Group I mainly includes the samples of U1 (except those deposited during major flood events) and some of the

samples of U2. These pyrogenic sources are confirmed by the same cross plot approach applied to the ULB bed sediment survey. FLT/202 and IcdP/276 range from 0.51 to 0.66 and from 0.35 to 0.57 along the river respectively. Furthermore, the ratio approach highlighted that downstream of the OFC (site Up8 to Do2), the bed sediments are characterized by  $0.56 < \text{FLT}/202 < 0.66$  and  $0.46 < \text{IcdP}/276 < 0.57$ , implying a major contribution of “aged” coal tar.

Finally, some other VIL2012 samples can be highlighted by a dominance of the contribution of “fresh” coal tar ( $\text{FLT}/202 = 0.56$ ;  $\text{IcdP}/276 = 0.64$ ; group II) as shown by the increase in the ratio IcdP/276 ( $> 0.57$ ). This specific signature is found in the oldest sample (128.5 cm) and in most contaminated sediments (113 and 84.5 cm) of U2, in samples deposited during the major floods and finally in the four particular samples (80.5, 58, 22.5 and 8.5 cm). The signature of the oldest and most contaminated sediments of U2 could be explained by a mixture between sediments deposited prior and after the end of the coking plant activities in the early 1980s, due to the reworking of sediments during the dam construction and the reservoir water filling operations. They could be mostly contaminated by water-leaching of coking and gas plants, which can result in a shift of the signal towards the “fresh” coal tar. Finally, the particular meteorological and hydrological conditions occurring during flood events could lead to intense erosion of nearby industrial soils and then to the reactivation of former contamination sources constituted by more preserved coal tar compared to “normal” conditions. The two particular samples excluded from the flood events (80.5 and 8.5 cm) have the same PAH signature even though its causes are difficult to elucidate. However, the high concentrations of BaP found in these particular levels could confirm the reactivation of contamination source derived from preserved coal tar.

## 4. Conclusion

A dated core sampled in the Villerest flood control reservoir located downstream of the OFC, provided crucial information for reconstructing a historical record of the PAHs contamination. The obtained data displays relatively high PAHs concentrations (1729–13349 ng/g) and then highly to very highly contaminated sediments. The total toxic BaP-equivalent (876–6290 ng/TEQ/g) associated to these contaminated levels could show potentially toxic effect and high carcinogenicity for biota via interstitial and surface water transfer by organic matter mineralization, reworking within pollutant-bearing phases transport and reservoir exploitation. The complementary data of the ULB bed sediments survey confirms the highest contamination just downstream of the OFC (2264–7460 ng/g). Typical 4-rings and 5-6 rings pyrogenic PAHs, such as FLT, PYR, BbF and BaP, were prevalent in ULB sediments. In some samples, BaP can represent up to 48% of the 16 priority PAHs. Since historical coal activities seem to strongly influence the PAH contamination through the exploitation of former coking or gas plants, these results confirm the use of BaP as a marker of coke production.

Finally, the diagnostic PAHs ratios approach pointed out major combustion-derived sources and suggests the dominance of mixed sources, especially derived from particles of urban and industrial air of Saint Etienne, with some contribution from “aged” coal-tar washout. The most recent sediments seem to be contaminated during uncontrolled runoff which can lead to industrial waste leaching such as oxidized coal tar and punctually by more preserved coal tar. In contrast, the oldest contamination could be linked to a mixture between sediments deposited prior and after the end of the coking plants activities in the early 1980s. Finally, specific hydro-sedimentary conditions occurring during flood

events result in the reactivation of former sources of contamination, related to more highly preserved coal tar.

As most of sediment studies are located in estuarine and coastal areas, these results contribute as supplementary record data in poorly described fluvial environments. Indeed, this study presents the first report of an environmental assessment of PAH contamination of the largest river in France and close to the most important coal district in France. It could be then helpful to better understand the environmental quality and the ecological resilience of aquatic systems close to major coal district in relation to hydro-sedimentary changes.

## Acknowledgments

The present work was performed as part of the research project “MetORG”, a collaboration between GeHCO, IC2MP and LMGE laboratories. It was supported by the Loire-Bretagne Water Agency. We thank all our collaborators, the LSCE laboratory and Irène Lefèvre for insights that contributed to the interpretation of the data. Finally, we thank Pr. Gan and the three anonymous reviewers for constructive suggestions to improve this manuscript.

## References

- Ayrault, S., Lefèvre, I., Bonté, P., Priadi, C., Carbonaro-Lestel, L., Mouchel, J.M., Lorgeoux, C., Djouarev, I., Gasperi, J., Moilleron, R., Tassin, B., 2008. Archives sédimentaires, témoignages de l'histoire du développement du bassin. <hal-00766529>.
- Barau, D., 2008. Les sources de l'histoire minière aux Archives départementales de la Loire. Documents pour l'histoire des techniques 16.
- Baumard, P., Budzinski, H., Garrigues, P., 1998. Polycyclic aromatic hydrocarbons in sediments and mussels of the western Mediterranean sea. *Environ. Toxicol. Chem.* 17, 765–776.
- Biache, C., Mansuy-Huault, L., Faure, P., 2014. Impact of oxidation and biodegradation on the most commonly used polycyclic aromatic hydrocarbon (PAH) diagnostic ratios: implications for the source identifications. *J. Hazard. Mater.* 267, 31–39.
- Blott, S.J., Pye, K., 2001. GRADISTAT: a grain size distribution and statistics package for the analysis of unconsolidated sediments. *Earth Surf. Process. Landf.* 26, 1237–1248.
- Budzinski, H., Jones, I., Bellocq, J., Piérard, C., Garrigues, P., 1997. Evaluation of sediment contamination by polycyclic aromatic hydrocarbons in the Gironde estuary. *Mar. Chem.* 58, 85–97.
- Carpentier, S., Moilleron, R., Beltran, C., Hervé, D., Thévenot, D., 2002. Quality of dredged material in the river Seine basin (France). II. Micropollutants. *Sci. Total Environ.* 299, 57–72.
- Cerniglia, C., 1992. Biodegradation of polycyclic aromatic hydrocarbons. *Biodegradation* 3, 351–368.
- Christensen, E.R., Bzdusek, P.A., 2005. PAHs in sediments of the Black River and the Ashtabula River, Ohio: source apportionment by factor analysis. *Water Res.* 39, 511–524.
- Choudhary, P., Routh, J., 2010. Distribution of polycyclic aromatic hydrocarbons in Kumaun Himalayan Lakes, northwest India. *Org. Geochem.* 41, 891–894.
- Cranwell, P.A., Koul, V.K., 1989. Sedimentary record of polycyclic aromatic and aliphatic hydrocarbons in the Windermere catchment. *Water Res.* 23, 275–283.
- Dahle, S., Savinov, V.M., Matishov, G.G., Evenset, A., Naes, K., 2003. Polycyclic aromatic hydrocarbons (PAHs) in bottom sediments of the Kara Sea shelf, Gulf of Ob and Yenisei Bay. *Sci. Total Environ.* 306, 57–71.
- Desmet, M., Mourier, B., Mahler, B., Van Metre, P., Roux, G., Persat, H., Lefevre, I., Peretti, A., Chapron, E., Simmoneau, A., Miège, C., Babut, M., 2012. Spatial and temporal trends in PCBs in sediment along the lower Rhône River, France. *Sci. Total Environ.* 433, 189–197.
- Dhivert, E., Grosbois, C., Coyne, A., Lefèvre, I., Desmet, M., 2015. Influences of major flood sediment inputs on sedimentary and geochemical signals archived in a reservoir core (Upper Loire Basin, France). *CATENA* 126, 75–85.
- Doong, R.-A., Lin, Y.-T., 2004. Characterization and distribution of polycyclic aromatic hydrocarbon contaminations in surface sediment and water from Gaoping River, Taiwan. *Water Res.* 38, 1733–1744.
- Duval, M.M., Friedlander, S.K., 1982. Source Resolution of Polycyclic Aromatic Hydrocarbons in the Los Angeles Atmosphere: Application of a CMB with First Order Decay. U.S. EPA Report EPA-600/2-81-161. U.S. Government Printing Office, Washington, DC.
- Fasnacht, M.P., Blough, N.V., 2002. Aqueous photodegradation of polycyclic aromatic hydrocarbons. *Environ. Sci. Technol.* 36, 4364–4369.
- Fernandes, M.B., Sicre, M.A., Boireau, A., Tronczynski, J., 1997. Polyaromatic hydrocarbon (PAH) distributions in the Seine River and its estuary. *Mar. Pollut. Bull.* 34, 857–867.
- Fernandes, M.B., Sicre, M.A., Broyelle, I., Lorre, A., Pont, D., 1999. Contamination by polycyclic aromatic hydrocarbons (PAHs) in french and european rivers. *Hydrobiologia* 410, 343–348.
- Fernandez, P., Vilanova, R.M., Martinez, C., Appleby, P., Grimalt, J.O., 2000. The historical record of atmospheric pyrolytic pollution over Europe registered in the sedimentary PAH from remote mountain lakes. *Environ. Sci. Technol.* 34, 1906–1913.
- Folk, R.L., Ward, W.C., 1957. Brazos River bar: a study in the significance of grain size parameters. *J. Sediment. Petrol.* 27, 3–26.
- Fu, J., Sheng, S., Wen, T., Zhang, Z.-M., Wang, Q., Hu, Q.-X., Li, Q.-S., An, S.-Q., Zhu, H.-L., 2011. Polycyclic aromatic hydrocarbons in surface sediments of the Jialu River. *Ecotoxicology* 20, 11.
- Gocht, T., Moldenhauer, K.-M., Püttmann, W., 2001. Historical record of polycyclic aromatic hydrocarbons (PAH) and heavy metals in floodplain sediments from the Rhine River (Hessisches Ried, Germany). *Appl. Geochem.* 16, 1707–1721.
- Grimalt, J.O., Van Drooge, B.L., Ribes, A., Fernandez, P., Appleby, P., 2004. Polycyclic aromatic hydrocarbon composition in soils and sediments of high altitude lakes. *Environ. Pollut.* 131, 13–24.
- Gu, H.G., Kralovec, A.C., Christensen, E.R., Van Camp, R.P., 2003. Source apportionment of PAHs in dated sediments from the Black River, Ohio. *Water Res.* 37, 2149–2161.
- Guo, J., Liang, Z., Liao, H., Tang, Z., Zhao, X., Wu, F., 2011. Sedimentary record of polycyclic aromatic hydrocarbons in Lake Erhai, Southwest China. *J. Environ. Sci.* 23, 1308–1315.
- Guo, J., Wu, F., Luo, X., Liang, Z., Liao, H., Zhang, R., Li, W., Zhao, X., Chen, S., Mai, B., 2010. Anthropogenic input of polycyclic aromatic hydrocarbons into five lakes in Western China. *Environ. Pollut.* 158, 2175–2180.
- Guo, Z., Lin, T., Zhang, G., Yang, Z., Fang, M., 2006. High-resolution depositional records of polycyclic aromatic hydrocarbons in the central continental shelf mud of the East China sea. *Environ. Sci. Technol.* 40, 5304–5311.
- Harrison, R.M., Smith, D.J.T., Luhana, L., 1996. Source apportionment of atmospheric polycyclic aromatic hydrocarbons collected from an urban location in Birmingham, U.K. *Environ. Sci. Technol.* 30, 825–832.
- Hinga, K.R., 2003. Degradation rates of low molecular weight PAH correlate with sediment TOC in marine subtidal sediments. *Mar. Pollut. Bull.* 46, 466–474.
- Itoh, N., Tamamura, S., Kumagai, M., 2010. Distributions of polycyclic aromatic hydrocarbons in a sediment core from the north basin of Lake Biwa, Japan. *Org. Geochem.* 41, 845–852.
- Jung, S., Chebbo, G., Lorgeoux, C., Tassin, B., Arnaud, F., Bonte, P., Winiarski, T., 2008. Temporal evolution of urban wet weather pollution: analysis of PCB and PAH in sediment cores from Lake Bourget, France. *Water Sci. Technol.* 57, 1503–1510.
- Karcher, W., 1988. Spectral Atlas of Polycyclic Aromatic Compounds, vol. 2. Netherlands, Springer.
- Ko, F.-C., Baker, J., Fang, M.-D., Lee, C.-L., 2007. Composition and distribution of polycyclic aromatic hydrocarbons in the surface sediments from the Susquehanna River. *Chemosphere* 66, 277–285.
- Laflamme, R.E., Hites, R.A., 1978. The global distribution of polycyclic aromatic hydrocarbons in recent sediments. *Geochim. Cosmochim. Acta* 42, 289–303.
- Landrum, P., Robbins, J.A., 1990. Bioavailability of sediment-associated contaminants to benthic invertebrates. In: Baudo, R., Giesy, J.P., Muntau, H. (Eds.), *Sediments; Chemistry and Toxicity of In-place Pollutants*. Lewis Publishers, Michigan, pp. 237–263 (Chap. 8).
- Lehr, R.E., Jerina, D.M., 1977. Metabolic activations of polycyclic hydrocarbons. *Arch. Toxicol.* 39, 1–6.
- Li, A., Ab Razak, I.A., Ni, F., Gin, M.F., Christensen, E.R., 1998. Polycyclic aromatic hydrocarbons in the sediments of the Milwaukee harbor estuary, Wisconsin, U.S.A. *Water Air Soil Pollut.* 101, 417–434.
- Li, G., Xia, X., Yang, Z., Wang, R., Voulvoulis, N., 2006. Distribution and sources of polycyclic aromatic hydrocarbons in the middle and lower reaches of the Yellow River, China. *Environ. Pollut.* 144, 985–993.
- Magi, E., Bianco, R., Ianni, C., Di Carro, M., 2002. Distribution of polycyclic aromatic hydrocarbons in the sediments of the Adriatic Sea. *Environ. Pollut.* 119, 91–98.
- Masclat, P., Bresson, M.A., Mouvier, G., 1987. Polycyclic aromatic hydrocarbons emitted by power stations, and influence of combustion conditions. *Fuel* 66, 556–562.
- Mc Elroy, A.E., Farrington, J.W., Teal, J.M., 1989. Bioavailability of PAH in the aquatic environment, metabolism of polycyclic aromatic hydrocarbons in the aquatic environment. In: Varanasi, U. (Ed.), *CRC Press, Boca Raton, Florida*, pp. 1–39.
- Mendonça, E., Picado, A., 2002. Ecotoxicological monitoring of remediation in a coke oven soil. *Environ. Toxicol. Chem.* 17, 74–79.
- Meyers, P.A., Ishiwatari, R., 1993. Lacustrine organic geochemistry – an overview of indicators of organic matter sources and diagenesis in lake sediments. *Org. Geochem.* 20, 867–900.
- Micic, V., Kruger, M.A., Hofmann, T., 2013. Variations of common riverine contaminants in reservoir sediments. *Sci. Total Environ.* 458–460, 90–100.
- Mourier, B., Desmet, M., Van Metre, P., Mahler, B., Perrodin, Y., Roux, G., Bedell, J.P., Lefèvre, I., Babut, M., 2014. Historical records, sources and spatial trends of PCBs along the Rhône river (France). *Sci. Total Environ.* 476–477, 568–576.
- Muniz, P., Danulat, E., Yannicelli, B., García-Alonso, J., Medina, G., Bicego, M.C., 2004. Assessment of contamination by heavy metals and petroleum hydrocarbons in sediments of Montevideo Harbour (Uruguay). *Environ. Int.* 29, 1019–1028.
- Pereira, W.E., Hostettler, F.D., Rapp, J.B., 1996. Distributions and fate of chlorinated pesticides, biomarkers and polycyclic aromatic hydrocarbons in sediments along a contamination gradient from a point-source in San Francisco Bay, California. *Mar. Environ. Res.* 41, 299–314.

- Peters, C.A., Knightes, C.D., Brown, D.G., 1999. Long-term composition dynamics of PAH-containing NAPLs and implications for risk assessment. *Environ. Sci. Technol.* 33, 4499–4507.
- Qiao, M., Wang, C., Huang, S., Wang, D., Wang, Z., 2006. Composition, sources, and potential toxicological significance of PAHs in the surface sediments of the Meiliang Bay, Taihu Lake, China. *Environ. Int.* 32, 28–33.
- Quantin, C., Joner, E.J., Portal, J.M., Berthelin, J., 2005. PAH dissipation in a contaminated river sediment under oxic and anoxic conditions. *Environ. Pollut.* 134, 315–322.
- Readman, J.W., Mantoura, R.F.C., Rhead, M.M., 1984. The physico-chemical speciation of polycyclic aromatic hydrocarbons (PAH) in aquatic systems. *Fresenius Z. Anal. Chem.* 319, 126–131.
- Rothermich, M.M., Hayes, L.A., Lovley, D.R., 2002. Anaerobic, sulfate-dependent degradation of polycyclic aromatic hydrocarbons in petroleum-contaminated harbor sediment. *Environ. Sci. Technol.* 36, 4811–4817.
- Sanders, M., Sivertsen, S., Scott, G., 2002. Origin and distribution of polycyclic aromatic hydrocarbons in surficial sediments from the Savannah river. *Arch. Environ. Contam. Toxicol.* 43, 0438–0448.
- Savinov, V.M., Savinova, T.N., Matishov, G.G., Dahle, S., Naes, K., 2003. Polycyclic aromatic hydrocarbons (PAHs) and organochlorines (OCs) in bottom sediments of the Guba Pechenga, Barents Sea, Russia. *Sci. Total Environ.* 306, 39–56.
- Simcik, M.F., Eisenreich, S.J., Lioy, P.J., 1999. Source apportionment and source/sink relationships of PAHs in the coastal atmosphere of Chicago and Lake Michigan. *At. Environ.* 33, 5071–5079.
- Soclo, H.H., Garrigues, P., Ewald, M., 2000. Origin of polycyclic aromatic hydrocarbons (PAHs) in coastal Marine sediments: case studies in Cotonou (Benin) and Aquitaine (France) areas. *Mar. Pollut. Bull.* 40, 387–396.
- White, K.L., 1986. An overview of immunotoxicology and carcinogenic polycyclic aromatic hydrocarbons. *Environ. Carcinog. Rev.* 4, 163–202.
- Witt, G., 1995. Polycyclic aromatic hydrocarbons in water and sediment of the Baltic Sea. *Mar. Pollut. Bull.* 31, 237–248.
- Xu, J., Guo, J.Y., Liu, G.R., Shi, G.L., Guo, C.S., Zhang, Y., Feng, Y.C., 2014. Historical trends of concentrations, source contributions and toxicities for PAHs in dated sediment cores from five lakes in western China. *Sci. Total Environ.* 470–471, 519–526.
- Xu, J., Yu, Y., Wang, P., Guo, W., Dai, S., Sun, H., 2007. Polycyclic aromatic hydrocarbons in the surface sediments from Yellow River, China. *Chemosphere* 67, 1408–1414.
- Yunker, M.B., Macdonald, R.W., 2003. Alkane and PAH depositional history, sources and fluxes in sediments from the Fraser River Basin and Strait of Georgia, Canada. *Org. Geochem.* 34, 1429–1454.
- Yunker, M.B., Macdonald, R.W., Vingarzan, R., Mitchell, R.H., Goyette, D., Sylvestre, S., 2002. PAHs in the Fraser River basin: a critical appraisal of PAH ratios as indicators of PAH source and composition. *Org. Geochem.* 33, 489–515.
- Zedeck, M.S., 1980. Polycyclic aromatic hydrocarbons: a review. *J. Environ. Pathol. Toxicol.* 537–567.